REPORTS OF PRACTICAL ONCOLOGY AND RADIOTHERAPY 24 (2019) 409–420

Available online at www.sciencedirect.com

ScienceDirect

journal homepage: http://www.elsevier.com/locate/rpor

Original research article

Estimation of radiation-induced second cancer risk associated with the institutional field matching craniospinal irradiation technique: A comparative treatment planning study

Hemalatha Athiyaman[a,*], *Athiyaman Mayilvaganan*[a], *Arun Chougule*[b], *Mary Joan*[b], *Harvinder Singh Kumar*[c]

[a] *Department of Radiological Physics, SP Medical College, Bikaner, Rajasthan, India*
[b] *Department of Radiological Physics, SMS Medical College, Jaipur, Rajasthan, India*
[c] *Department of Radiotherapy, SP Medical College, Bikaner, Rajasthan, India*

ARTICLE INFO

Article history:
Received 15 January 2018
Received in revised form
6 April 2019
Accepted 18 June 2019
Available online 8 July 2019

Keywords:
Second cancer
Craniospinal irradiation
Organ equivalent dose
BEIR
Field matching

ABSTRACT

Aim: To estimate and compare the lifetime attributable risk (LAR) of radiation-induced second cancer (SC) in pediatric medulloblastoma patients planned with institutional 3D conformal field matching method, gap junction method and Intensity Modulated Radiotherapy (IMRT).

Background: The epidemiological studies on childhood cancer survivors reported that long-term cancer survivors who received radiotherapy are at a significantly increased risk for the development of SC. Hence, the increased concern to predict the SC risk for long-term survivors.

Materials and methods: In addition to institutional field matching planning method, IMRT and gap junction methods were created for ten pediatric medulloblastoma patients. The risk estimates were made based on the site-specific cancer risk coefficient provided by the BEIR VII committee according to the organ equivalent dose for various critical organs. Also, plans were compared for target volume dose distribution and dose received by critical organs.

Results: When compared to the gap junction method, the IMRT and institutional field matching method were superior in normal tissue sparing and dose conformity. However, highly significant volume of low dose associated with IMRT was the main concern for the SC risk. The accumulated LAR for all the critical organs with 3D conformal gap junction and IMRT method was 23–25% while for the 3D conformal field matching method it was 21%.

Conclusion: The LAR associated with the institutional field matching technique was substantially lower. As this method is highly robust and easy to set up, it can be a better choice of a craniospinal irradiation technique where 3DCRT is the only choice of treatment.

* *Corresponding author.*
E-mail addresses: hemathi@gmail.com (H. Athiyaman), athiyaman.bikaner@gmail.com (A. Mayilvaganan), arunchougule11@gmail.com (A. Chougule), joanmkunnel@gmail.com (M. Joan), drkumarhs@gmail.com (H.S. Kumar).
https://doi.org/10.1016/j.rpor.2019.06.004

1. Background

The most common primary malignant tumor of the Central Nervous System (CNS) during childhood is medulloblastoma. It is most likely to develop in the posterior fossa during pediatric years. Among all childhood brain tumors, medulloblastoma comprises approximately 25% of all cases and is mostly diagnosed between the age of 5 and 9 years.[1–4] Medulloblastoma is relatively chemo-radiosensitive; hence, radiotherapy (RT) along with surgery and chemotherapy improves the survival of patients. As medulloblastoma typically arises in the posterior fossa and has a predisposition to invade the subarachnoid space of the CNS through the cerebrospinal fluid, craniospinal irradiation (CSI) along with a posterior fossa boost has become the standard treatment for medulloblastoma since the late 1960s.[5]

The use of RT is associated with better outcomes in many pediatric cancer patients, but it is also associated with significant long-term adverse effects including cardiopulmonary impairment, loss of hearing or vision, neurocognitive defects, endocrine system dysfunction, gonadal dysfunction, and risk of second cancer (SC) due to dose delivered to healthy tissues.[6–13] Even though the risk of RT patients developing SC is small, it is statistically significant. It has different histology compared to the original disease. Hence, it is necessary to compare RT treatment plans in order to minimize SC induction. There have been many conformal RT techniques introduced to treat very large and complex shaped target volumes in CSI. The classical or traditional way of treatment method is a single posterior spine field combined with the bilateral cranial field. In order to avoid over or under dose in the field matching areas either radiation fields are abutted or a gap is introduced and the junction shifted in regular intervals. In our institute, for CSI, a simple 3D conformal field matching technique using a field alignment option has been adopted since 2014. The field alignment option in the eclipse treatment planning system simply calculates the necessary collimator, couch, and gantry angle to match the diverging planes of both fields. This study focuses on comparing this institutional field matching technique with traditionally used gap junction method and IMRT with respect to late adverse effects, particularly radiation-induced SC.

Among childhood cancer survivors, patients with CNS tumors have a higher risk of SC in the brain and body due to CSI, compared to other childhood malignancies.[14] Moreover, an increased risk of SC has been observed in pediatric cancer patients after chemotherapy and RT, compared to a general population.[15–18] These adverse effects may be observed decades after the treatment. Cancer survivors have an increased risk even at 30–40 years after initial treatment.[19] But the latency period does not exceed the life expectancy for pediatric patients. This makes the SC risk a main concern for pediatric patients. The young patients are prone to carcinogenic effects due to greater radiation effects in the period of rapid cell proliferation. Hall et al. have given three major factors that contribute to an increased risk of SC. First, based on an atomic bomb survivor study, it has been found that cancer risk depends on age at exposure. So, it has been quoted that the radiation-induced cancer risk for all ages is 5% per Sievert (Sv), which decreased to 1% per Sv for mature adults and those 60 years of age and older. The second factor is a germ line mutation involved in childhood cancer which includes increased radio sensitivity to radiation-induced cancer. Finally, in a child, the radiogenic organs are closer to treatment site than in an adult due to the difference in body size which also results in significant whole-body scatter dose. One example of the sensitivity of children is a high incidence of breast cancer development in patients treated for Hodgkin's lymphoma at young age.[20] In another childhood cancer survivor study, Friedman et al. revealed valuable information on the late adverse effects after the treatment of pediatric cancer. This study included 20,346 childhood cancer survivors and showed a 20.5% higher incidence of subsequent SC after 30 years of diagnosis in patients who received RT.[21] However, these adverse effects can be reduced if the volume of normal tissue irradiated during RT treatment is kept to a minimum.

Over the past decades, advancement in the treatment of pediatric cancer has increased the 5-year survival rate of patients from 30% to 80%.[22] However, along with the improvement in survival, childhood cancer survivor studies have also reported an increase in treatment-related health problems such as SC. The risk of SC has significantly increased in long-term childhood cancer survivors who live long enough to develop SC after the treatment.[23,24] To reduce the adverse effects associated with RT, the absorbed dose to the craniospinal axis should be reduced. Currently, owing to the combination of chemo-radiotherapy, the total prescribed dose for the craniospinal axis has been reduced to 23.4 Gray (Gy) from 36 Gy; this is possible because tumor control with a combination of chemotherapy and 23.4 Gy CSI is similar to that obtained with 36 Gy. To reduce the incidence of SC due to RT, various new techniques using protons and heavy ions have also been proposed. However, only a limited number of studies have estimated the risk of SC after 3D conformal techniques compared to contemporary treatment techniques, such as IMRT, Intensity Modulated Proton Therapy (IMPT), rapid arc and electron therapy. In these studies, the 3D-conformal method used for the comparison is the traditional gap junction technique (gap between the field edges) with feathering, and most of the study results have shown to favor IMPT over photon therapy due to substantial sparing of the normal tissue.[25] Thus, no study has been able to obtain complete information on SC risk associated with 3D conformal matched fields in comparison with the traditional 3D conformal gap junction and IMRT techniques.

This study retrospectively compared Planning Target Volume (PTV) dose distribution, dose received by critical organs and the risk of SC associated with the institutional 3D conformal field matching technique with that of the traditional 3D conformal gap junction and IMRT technique for CSI in pediatric patients with medulloblastoma. The radiation-induced SC risk was evaluated for the critical organs inside and adjacent to the spinal field for which the Biological Effects of Ionizing Radiation (BEIR) VII phase II Committee has provided lifetime risk estimates.[26]

2. Materials and methods

For the dosimetric and SC risk assessment, 10 pediatric patients (mean age: 9 years; age range: 5–16 years; two girls and eight boys) treated with the institutional 3D conformal field matching technique were selected.

2.1. Planning methods

The 3D conformal field matched, gap junction and inverse IMRT plans were created in the TPS for the prescribed dose of 23.4 Gy in 1.8 Gy per fraction. The 3D and IMRT dose calculation was performed by using the anisotropic analytical algorithm (AAA) and photon optimizer algorithm, respectively, for 6 MV photon beams, delivered by Varian Clinac 2300 CD (Palo Alto, US) linear accelerator. The three planning methods used are described below:

2.1.1. Method 1: Institutional 3D conformal matched fields

The half beam-blocked cranial and cervicothoracic spinal fields created for cranium and upper spine; which obviated the necessity of a collimator and couch rotation as well as the uncertainty due to beam matching in the most sensitive cervical spine region. The remaining lumbosacral spinal field was planned with the posterior symmetrical field. Following that, the superior diverging end of the lumbosacral field was matched with the inferior diverging end of the lumbosacral field by using a field alignment option that calculates and automatically applies the necessary gantry, collimator, and couch rotation to the fields. The dosimetric uncertainty due to a systematic or random setup error was eliminated by auto sequencing the junction. The junctions were sequenced in a caudal direction by changing the field size without altering the isocenter.[27]

2.1.2. Method 2: IMRT

Inverse IMRT planning was performed for the posterior spinal field. Three posterior spinal fields (20–45°), which encompass the whole spine with gantry angle zero, were created. Inverse optimization was performed to achieve 95% dose coverage for the entire PTV and to reduce the dose to the critical organs within the tolerance limit.

2.1.3. Method 3: Traditional 3D conformal gap junction method

Similar to method-1, the half beam-blocked cranium and cervicothoracic spinal fields were created. Then, the inferior edge of the cervicothoracic and superior edge of the lumbosacral fields were allowed to diverge on the skin. Both these field edges were separated by a gap distance S. The distance S was calculated individually for every patient in such a way that both diverging edges were matched at the depth of the spine. To achieve a uniform distribution within the PTV, the junction was feathered in the caudal direction by 1 cm. The gap distance, S, was calculated and applied for every junction shift.

The formula for calculating the gap S is

$$S = S_1 + S_2,$$

where $S_1 = 0.5 \times L_1 \times (d/\mathrm{SSD}_1)$, where L_1 is the field length, SSD_1 is the source to surface distance of the cervicothoracic field, and d is the depth of the spine. $S_2 = 0.5 \times L_2 \times (d/\mathrm{SSD}_2)$, where L_2 is the field length, SSD_2 is the source to surface distance of the lumbosacral field, and d is the depth of the spine.

2.2. Dosimetric comparison

The dosimetric comparison among the three planning methods was performed for PTV dose distribution and critical organ dose. The dose distribution with planning details is shown in Fig. 1. The PTV dose distribution was analyzed by calculating $D_{\max}$, D_{mean}, Homogeneity Index (HI), Vants Riet Conformity Index (CI), and volume receiving 107% and 95% of the dose ($V_{107\%}$ and $V_{95\%}$, respectively). The ideal value for HI is zero and for CI is one.

$$\text{Formula for HI} = \frac{D_5 - D_{95}}{D_{\mathrm{P}}}$$

where D_5 – dose to 5% of the volume, D_{95} – dose to 95% of the volume, and D_{P} – prescribed dose.

$$\text{Formula for Vants Riet CI} = \frac{\mathrm{TV_{ri}} \times \mathrm{TV_{ri}}}{\mathrm{TV_{ri}} \times V_{\mathrm{ri}}},$$

where $\mathrm{TV_{ri}}$ – treatment volume receiving the reference isodose and V_{ri} – volume receiving the reference isodose.

The dose to the critical organs was evaluated by the volume receiving 80%, 50%, 30% and 10% of the prescribed dose, $D_{\max}$ and D_{mean} parameters.

2.3. Second cancer risk estimation

Over the last ten years, the radiation associated risks have noticeably increased with a significant increase in the use of ionizing radiation in medical imaging and cancer treatment. Studies of these patients have provided important information for understanding the radiation risk, particularly breast and thyroid. Some authors have predicted thousands of radiation-induced cancer cases in the US population in the coming years.[28] Nearly 14,500 cancer deaths were predicted from CT examinations. Brenner and Hall estimated that in the US CT scan is responsible for 1–2% of all future cancer cases.[29] Based on this prediction and several other reports, a committee was formed to assess the health risk from a low level of ionizing radiation under the national academy of sciences. The most recent report published by the committee is the Biological Effects of Ionizing Radiation (BEIR) VII phase 2 issued in 2006.

The atomic bomb survivors, individuals medically exposed and radiation accidents are the basic source of knowledge for radiation-induced cancer. Based on this data, the radiation protection bodies (BEIR VII 2006, United Nations Scientific Committee on the Effects of Atomic Radiation Effects of ionizing radiation (UNESCAR 2006)) have developed various dose–response relationships for carcinogenesis. And these reports found that the linear dose–response model is not valid for all solid cancers. This finding is supported by the increasing trend observed for radiation-induced leukemia in dose–response relation. It is also observed that the dose–response relationship follows a linear pattern when the absorbed dose is below 2 Gy. It is based on the assumption

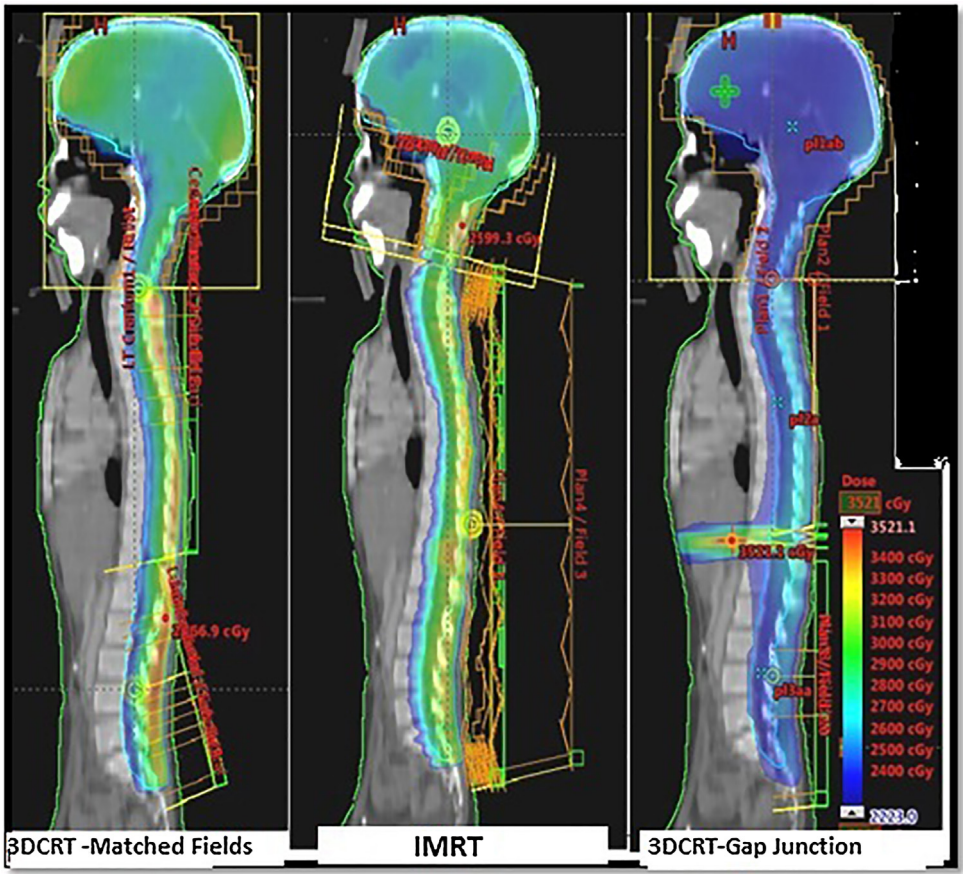

Fig. 1 – Dose distribution for the three planning methods.

that a single particle may cause a mutation in a single cell. For a dose greater than 2 Gy, sterilization effects become more important than mutation effects; therefore, the radiation-induced cancer incidence may not be proportional to the mean dose for dose greater than 2 Gy.[30] In the medium to high dose region (>2.5 Gy) induction of cancer is very rare so it is difficult to get parameterization. At the high dose range, typically above 5 Gy, the dose–response relationship is not well known and it has been reported that it could be linear, bell-shaped due to cell kill or plateau-shaped due to a balance between repopulation and cell kill and also different for particular organ types. As long as cell repopulation is small, cancer induction shows a bell-shaped behavior as an extensive repopulation plateau shape is approached.[31]

In patients who receive RT as a part of curative treatment, some parts of the organ receive a low to high inhomogeneous dose, which must be taken into account instead of the mean dose for the SC risk estimation. Indeed, most previous studies have evaluated the SC risk based on the mean dose. To account for the inhomogeneous dose distribution while estimating SC risk, the concept of organ equivalent dose (OED) was introduced by Schneider et al. By definition, OED is a dose (Gy), and any dose distribution in an organ is equivalent and corresponds to the same OED if it causes the same radiation-induced cancer incidence.[32] Where the dose distribution is broken up into N equal voxels and the cell sterilization parameter is applied for every voxel. OED corresponds to an average organ dose for a low dose region. While for a medium to high dose region, the OED accounts for the impact of cell killing. The cell killing effect is taken into account as an exponential function in the linear exponential dose–response relation and that depends on the dose and organ-specific cell sterilization parameter. When applying the OED concept, the major difficulty was to define the organ-specific cell sterilization parameter (α) for each organ. Since the Hodgkin cancer patients are young, treated with curative intent and SC incidence rates for various organs were known, the data of these patients became ideal to find the alpha value. Although the RT treatment for Hodgkin's patient was very successful, neither the time of treatment nor the institutional protocol had much impact on the treatment techniques or prescription.[33] So the effect of cell sterilization was estimated based on SC incidence data of Hodgkin patients who were treated with RT in the period of 1962–1993.[34] In 2011 Schneider presented the site-specific dose–response relationship for RT dose range by combining the Linear No-threshold model derived from the atomic bomb survivors study and from Hodgkin cohort treated with RT.[35]

For Schneider's OED calculation, the 3D dose distribution data is necessary; which is not available in the epidemiological studies. Hence, the dose volume information for various organs, such as the lungs, bladder, thyroid, colon, liver, and stomach was extracted from differential dose volume histograms. From the dose volume relation, OED was calculated

for the linear, bell-shaped, and plateau dose–response models using Eqs. (a)–(c):

$$\mathrm{OED}_{\mathrm{linear}} = D_{\mathrm{mean}} = \int D dv \quad \text{(a)}$$

$$\mathrm{OED}_{\mathrm{bellshape}} = \int D e^{-\alpha D} dV \quad \text{(b)}$$

$$\mathrm{OED}_{\mathrm{plateau}} = \int \frac{1 - e^{-\delta_{\mathrm{org}}}}{\delta_{\mathrm{org}}} \mathrm{Di} dV \quad \text{(c)}$$

where V is the whole structure volume, Di is the dose element, α and δ_{org} are the organ-specific model parameters, as described by Schneider et al.[32,34] The organ-specific model parameters were tabulated by Schneider by fitting the above dose–response relationships of various organs into OED data and to the atomic bomb survivors.

To generate the appropriate risk models and factors to apply for cancer risk estimation, the BEIR VII committee relied on analysis of atomic bomb survivors done by the Radiation Effects Research Foundation (RERF). The committee developed two competing risk models that are Excess Relative Risk (ERR) and Excess Absolute risk (EAR) model. The ERR is the rate of disease in an exposed population divided by the rate of disease in an unexposed population. The EAR is the difference between the exposed population and an unexposed population. Both models can be used to calculate the lifetime risk of SC based on the age at the time of exposure and sex. In order to calculate the lifetime risk, the BEIR VII committee introduced the third model called lifetime attributable risk. The LAR is nothing but the summation of EAR or ERR calculated for each year following exposure to an expected life span of 80 years. It is dependent on age at exposure and sex of the subject and includes a latency period from exposure to the first risk of cancer (5 years for solid cancers) and dose and dose rate effectiveness factor (DDREF). The DDREF factor accounts for the reduction of ionizing radiation effects of low dose and low dose rate when compared to high and high dose rates. This factor helps to merge the medium to high dose epidemiological data with the low dose animal epidemiological data for which the BEIR committee suggests the value of 1.5 for all solid tumors.[28] From the calculated OED, the lifetime attributable risk (LAR) – the probability for an individual to develop cancer associated with exposure was estimated using the parameters given in BEIR VII phase 2 report.[26] This was published in 2006 and developed the best possible risk estimate for human exposure to low dose, low linear energy transfer radiation. It suggests a straight line relationship between radiation dose and induced cancer risk only at low dose levels. The advantage of this model is that it includes gender and organ-specific parameters as well as takes into account age at exposure and attained age since exposure. Even though various nonlinear risk models are available for estimating SC risk, BEIR VII model is considered reasonable for risk estimation for out of field organs in RT since it receives a low dose. The LAR for each organ was calculated based on the linear, plateau, and bell-shaped dose–response models using the following equation:

$$\mathrm{LAR} = \mathrm{OED} \times R$$

The risk coefficient, R, taken from BEIR VII phase 2 reports, corresponds to each patient, type of organ, and age of exposure. It is a combined estimate based on absolute and relative risk transport and has been adjusted by a DDREF 1.5. The calculated LAR for childhood cancer patients refers to the risk of developing malignancies to the particular organ at any time after RT.[26]

2.4. Statistical analysis

The differential dose volume histogram data were extracted for all the plans. The mean value for dosimetric parameters and OED was calculated. Statistical analysis was performed with SPSS 20 software, version 20 (Statistical Package for the Social Sciences, IBM Corporation, Armonk, New York, US). The paired *t*-test was used for comparing mean doses to critical organs and PTV dosimetric parameters. For OED, the error bar is plotted with 95% confidence interval and paired *t*-test is performed to find the statistical significance. The *p*-value less than 0.05 was considered as statistically significant.

3. Results

The PTV dose distribution and the dose to the critical organs for three different planning methods were compared and statistically analyzed. The maximum dose was significantly higher with the 3D conformal gap junction method ($p < 0.001$). Both $V_{95\%}$ (p – 0.044) and $V_{107\%}$ (p – 0.001) were significantly higher with the IMRT plan than 3D conformal matched field. The difference in the HI among the three planning methods was not significant. The CI results were better with the IMRT plan; however, the difference was not significant. Overall, the PTV dose distribution of 3D conformal field matching planning method was comparable to IMRT.

3.1. OAR parameters

The dose to critical organs was analyzed with $V_{80\%}$, $V_{50\%}$, $V_{30\%\ \mathrm{and}}$ $V_{10\%}$. As shown in Table 1, the high dose volumes, such as $V_{80\%}$ and $V_{50\%}$, were lower with IMRT compared to 3D conformal field matching plans for most of the critical organs. Except for the liver in the gap junction method, the low dose volumes ($V_{30\%}$ and $V_{10\%}$) were reduced by the 3D-conformal methods as compared to IMRT for all the organs. The dose to the liver was significantly lower (p – 0.05) with 3D conformal matched field plan compared to the 3D conformal gap junction plan, especially $V_{30\%}$ because the gap junction for some patients arises in the liver region.

As shown in Fig. 2, the mean dose to the heart was significantly lower with the IMRT plan (p – 0.0018) compared to 3D conformal field matching plan. The 3D conformal gap junction method delivered a significantly higher mean dose to the liver (p – 0.008) and stomach (p – 0.018) as compared to 3D conformal matched field method. The mean dose to the bladder was significantly reduced with the IMRT plan as compared to the

Table 1 – Dose statistics for organ at risk.

Organ	$V_{80\%}$			$V_{50\%}$			$V_{30\%}$			$V_{10\%}$		
	Method: 1	Method: 2	Method: 3	Method: 1	Method: 2	Method: 3	Method: 1	Method: 2	Method: 3	Method: 1	Method: 2	Method: 3
Left eye	21.93	25.49	26.18	33.6	56.91	46.47	53.4	73.53	62.57	87.45	89.98	98.32
Right eye	13.96	16.29	14.94	27.36	43.5	33.98	40.23	59.8	48.52	81.61	89.9	93.92
Heart	15.98	3.43	20.99	66.9	33.63	68.44	70.73	66.62	71.4	80.45	94.38	82.7
Right lung	13.42	4.44	12.5	21.78	13.89	20.4	25.46	28.12	23.83	42.81	56.34	41.96
Left lung	7.65	2.45	7.81	12.16	8.99	12.33	30.5	19.49	15.04	28.11	48.05	28.99
Thyroid	52.3	48.03	60.09	78.46	96.77	78.98	85.24	99.74	85.21	100	100	100
Right kidney	10.73	3.11	11.74	17.85	9.83	17.82	22.92	19.22	22.63	43.02	60.14	45.43
Left kidney	8.08	3.5	8.7	14.38	9.66	13.53	18.94	18.47	18.11	36.93	56	39.02
Liver	6.61	1.32	11.83	29.81	16.03	31.7	32.95	38.07	34.07	41.27	59.28	44.83

Method 1 – 3D conformal field matching method (institutional), Method 2 – IMRT, Method 3 – 3D conformal gap junction method. V_{80}, V_{50}, V_{30}, V_{10} – volume receiving 80%, 50%, 30%, 10% of prescribed dose given in percentage.

Table 2 – Organ equivalent dose (OED) for various critical organs.

Organ	Linear dose response (OED, Gy)			Bell-shaped dose response (OED, Gy)			Plateau-shaped dose response (OED, Gy)		
	3D-matched field	IMRT	3D-gap junction	3D-matched field	IMRT	3D-gap junction	3D-matched field	IMRT	3D-gap junction
Right lung	5.83	5.59	5.32	1.32	1.75	1.38	2.38	2.87	2.74
Left Lung	3.89	3.78	4.22	1.25	1.66	1.29	1.91	2.39	2.31
Colon	7.05	6.663	7.2	0.73	0.932	0.85	2.17	2.58	1.97
Thyroid	16.38	17.99	16.49	9.0511	9.88	7.96	1.45	1.38	1.34
Stomach	3.48	3.62	3.49	1.16	1.57	1.22	0.54	0.88	0.71
Bladder	11.2	4.3	5.8	0.05	0.07	0.1	0.18	0.28	0.19
Liver	6.17	5.82	6.95	0.38	0.42	0.36	0.68	0.74	0.711

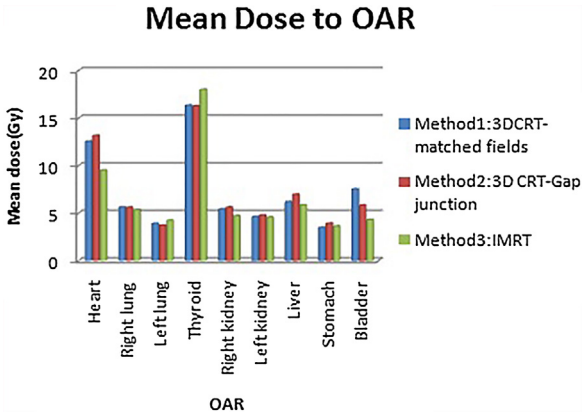

Fig. 2 – Mean dose to the organ at risk (OAR).

3D conformal matched field (p – 0.0012); in the field matching plan, due to an oblique incidence of a lower spinal field, it encompassed more volume of the bladder than IMRT; however, the difference was not significant in comparison with the gap junction method. Even though IMRT reduced the mean dose to critical organs, the low dose volume which contributes to integral dose was higher when compared to 3D-conformal methods.

3.2. *Second cancer risk analysis*

The results of OED for various organs with statistical significance are shown in Figs. 3–5. In general, for all the organs, the highest risk on the basis of OED was found with the linear dose–response model, and a lower risk was associated with the bell-shaped and plateau models Table 2.

Analysis with the plateau dose–response model (Fig. 3) showed that the 3D conformal institutional matched field method was associated with significantly lesser OED for the lung (p – 0.012), liver (p – 0.011), colon (p – 0.046) and stomach (p – 0.026) than the IMRT technique; similarly, with the 3D conformal gap junction method for the lung (p – 0.034) and liver (p – 0.027). For the bladder and thyroid, the plateau models showed an insignificant difference between 3D conformal matched field and IMRT plans. For other organs, it showed an insignificant difference between the three methods.

The bell-shaped model also predicted that the matched field method was associated with significantly lesser OED as compared to IMRT for the lungs (p – 0.001), bladder (p – 0.017), colon ($p < 0.0001$), and stomach (p – 0.002). This model also showed an insignificant difference between the 3D conformal gap junction and field matching methods for all the organs, except the bladder (p – 0.025) (Fig. 4).

The linear model (Fig. 5) showed that the difference among all the three planning methods for the lungs, colon, and thyroid was not significant. For the bladder, the linear model predicted that the 3D conformal matched field method was associated with a significantly higher OED than IMRT (p – 0.001) and 3D conformal gap junction method (p – 0.008) owing to an oblique incidence which delivers higher mean dose to the bladder than the other two methods. For the liver, OED associated with the 3D conformal field matching method was significantly lower than the gap junction method (p – 0.008). An exception was seen for the thyroid with a larger OED, as well as a larger mean dose because of its presence in the exit dose region of the spinal field for some patients.

Finally, as per the nonlinear model, IMRT contributed to a maximum OED when compared to matched field method for most of the organs. Specifically, the lung and colon contributed the most. The difference between nonlinear models was due to cell killing and repopulation effects.

The overall impact of the three planning methods and the nominal LAR for all the patients are presented in Fig. 6.

The LAR calculated using BEIR VII parameters favored the matched field method for most of the organs in all the patients. Our results showed that the risk of SC was higher for the colon, thyroid, and bladder according to the linear dose–response model for all the three planning methods. As OED is directly proportional to the mean dose, a higher mean dose resulted in a higher risk. And this model is valid for a dose range up to 2 Gy and uniformly irradiated. For the dose greater than 2 Gy, the effect of cell killing is not accounted as, indeed, dead cells cannot undergo malignancy or mutation.

According to the bell-shaped model, the IMRT technique was associated with a substantially higher risk when compared to the other 3D-conformal methods. The risk calculation based on the plateau model also favored the 3D conformal matched field method. The accumulated risk of all organs based on the plateau model for the 3D conformal gap junction and IMRT was 23–25%, while the corresponding value for the 3D conformal matched field method was 21%.

4. Discussion

Many dosimetric studies have been performed in the junction region to evaluate the effect of gap and feathering. The dosimetric behavior of matched, overlapped, and gap junction methods has been studied for Co-60 and 4 MV photon beam by Tatcher et al. The study resulted in a homogeneous and smooth dose distribution for a matched field, and the gapped junction resulted in under dosing with inhomogeneous dose distribution.[36] Also, the film dosimetry in the moving gap region was performed by Cheng et al. with various ranges of feathering. For a 0.5-cm gap and 1-cm feathering step size, the dose varies from 82% to 88% of the brain field, and for a 1-cm gap and 1-cm feathering, the corresponding dose varies from 68% to 73% in the gap junction region. Finally, with no gap and 1-cm feathering step, the dose varies from 92 to 98%.[37] The dose inhomogeneity effect of the gap junction has also been confirmed by Holupka et al.[38] Similarly, the dosimetric comparison performed in this study favored the institutional matched field method for a homogeneous dose distribution in the junction.

The dosimetric comparison between the 3D conformal RT (3D-CRT) and IMRT-linac and IMRT-tomotherapy has been performed by Sharma et al. in 2009. The study demonstrated a better dose in terms of coverage and conformity with the IMRT-tomotherapy and linac plans than 3D-CRT. Furthermore, this study showed that the high dose volumes of the critical organs were lesser with the IMRT plan than with 3D-CRT. However, the low dose volumes that contribute to the SC risk are higher

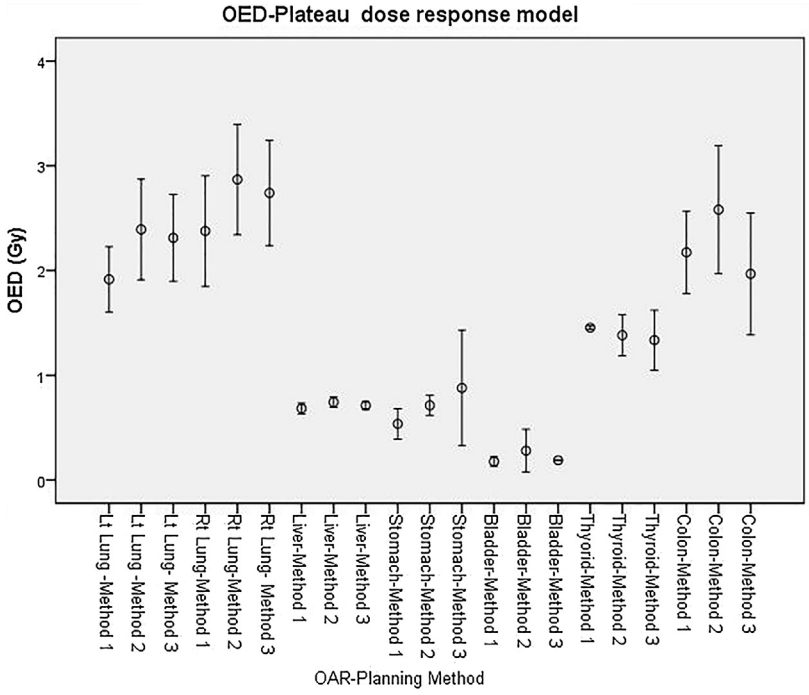

Fig. 3 – Organ equivalent dose calculated by plateau model for the selected OAR (Method 1 – 3D conformal matched field; Method 2 – IMRT; Method 2 – 3D conformal gap junction).

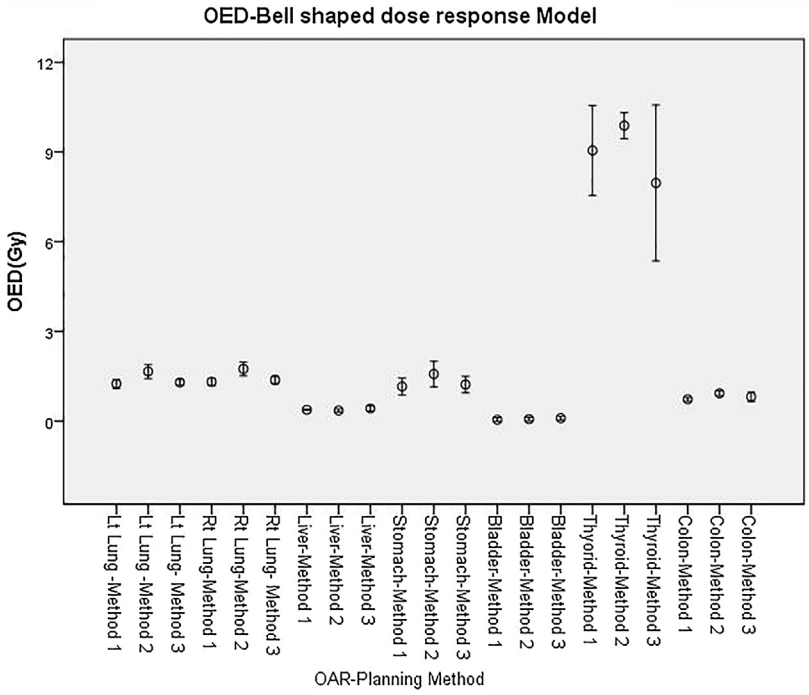

Fig. 4 – Organ equivalent dose calculated by bell-shaped model for the selected OAR (Method 1 – 3D conformal matched field; Method 2 – IMRT; Method 3 – 3D conformal gap junction).

with IMRT plans.[39] Similarly, in our current study, we found that the dose coverage and critical organ sparing were better with IMRT compared to the 3D-conformal methods. However, the low dose volumes $V_{30\%}$ and $V_{10\%}$ of the critical organs were found to be lower with 3D-conformal methods than IMRT.

Radiobiological and SC risk associated with the photon and proton therapy have been studied by Brodin et al. in 2011. The plan comparison was retrospectively performed for 10 patients with pediatric medulloblastoma, and OED for the plateau model was calculated and applied for estimating

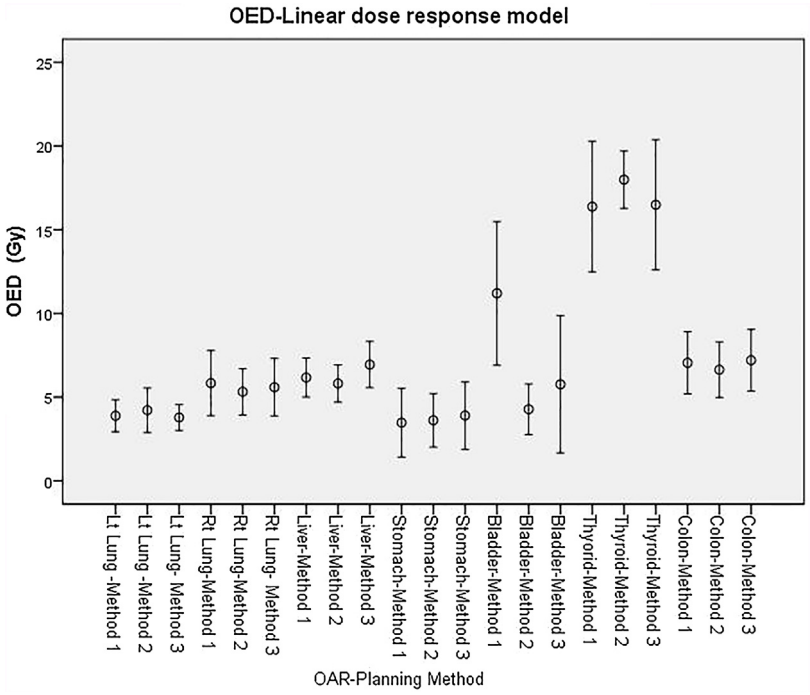

Fig. 5 – Organ equivalent dose calculated by linear dose response model for the selected OAR (Method 1 – 3D conformal matched field; Method 2 – IMRT; Method 3 – 3D conformal gap junction).

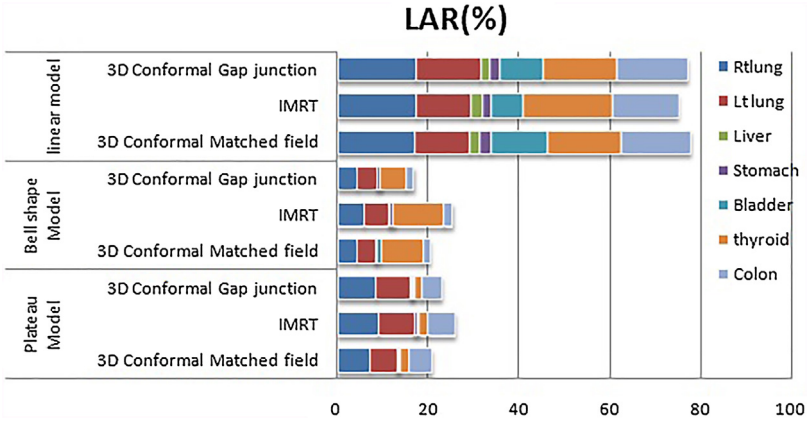

Fig. 6 – The percentage of total lifetime attributable risk of second cancer for the three planning methods by all models.

the SC risk. Among noncancerous adverse effects, the incidence of serious late complications, such as heart failure, was higher with 3D-CRT compared to IMRT. The SC risk estimation showed that IMRT plans were associated with a higher risk compared to 3D-CRT plans.[33] Similarly, the calculated OED and SC risk of our study were in accordance with those obtained in the study by Brodin et al. Using a prescription dose of 23.4 Gy, Mu et al. also estimated the lifetime risk of lethal SC and found that the risk was 20% with 3D-CRT and 30% with IMRT.[40] The following factors must be considered before replacing 3DCRT with IMRT. The first one is a higher number of monitor unit delivery results in a higher total body dose. Secondly, a larger volume of low dose regions due to more fields applied. Kry et al. also studied various linear accelerators for different energies and concluded that the leakage radiation may vary a little but IMRT would double the risk of induced SC in long-term survivors due to more monitor units.[41]

The SC risk estimation after pediatric CSI with an electron, photon, and proton therapy was studied by Stokkevag et al. They also included OED calculation, and the LAR was calculated using the BEIR VII committee model for estimating the age- and site-specific incidence of SC based on OED. The study results showed a significant risk of SC in the thyroid, lungs, and colon, as compared to the stomach, after electron and photon treatment. With proton therapy, the risk of SC in all the organs, except the lungs was reduced to the minimum. In their study population, the organs, such as the thyroid, colon, and lungs, were shown to contribute highly to the total risk from all the techniques.[42] Similarly, in the present study, the LAR calculated for the lungs, colon, and thyroid based on the BEIR VII model contributed the most to the total risk.

The robustness of the treatment techniques is also an important factor. The junction between the field edges may result in a risk of overdosing or underdosing owing to uncertainties in the treatment setup. With the advent of modern techniques, these problems can be resolved. However, in most centers, 3D-CRT is still the choice of treatment for medulloblastoma. In this context, our institutional 3D conformal field matching method is highly robust owing to its simple setup with two isocenter for a larger spine, Multi-Leaf Collimator (MLC) segments for a homogeneous dose distribution, and computerized junction auto sequence with a record and verification mode of delivery. The dose to critical organs and estimated LAR of SC were also found to be lower with this technique when compared to the traditional 3D conformal gap junction method. So the field matching planning method can be used safely for CSI where 3DCRT is the choice of treatment method.

The shape of dose–response relationship which is underlying the OED is not precisely known. Based on animal studies, Mole reported that the shape of linear exponential or quadratic exponential dose–response relationship was supported by the cancer incidence data after whole-body exposures of animals.[43] The advantage of the animal studies is a homogeneous dose exposure to each organ as it is irradiated homogeneously. On the other hand, the analysis of the average dose in the patient who developed radiation-induced bladder cancer following radiotherapy for adjacent tumors results in a plateau dose–response relationship.[34] Similarly, Wheldon and Lindsay applied two stage mutation models to obtain a dose–response curve for radiotherapy dose range. At 20 Gy they found that cancer risk vanished and the relation became bell-shaped.[44] Another approach was based on the epidemiological data of the atomic bomb survivors done by Schneider and Walsh. They extended the study to two extra high dose categories by combing the cancer data of Hodgkin's patients. This work resulted in bending over of the dose–response curve for a dose greater than 2 Gy. From this work, they concluded that if the fraction effect is not considered then the dose–response curve will show a bell-shaped behavior due to the cell sterilization effect at the high dose. When the repopulation effect is present due to fractionation then a plateau dose–response should be considered.[45] Further experimental work is necessary to quantify the effect of the dose–response relationship at high doses.

According to the linear dose–response model, the mean dose to an organ should be reduced to decrease the risk of radiation-induced cancer. Because OED is directly proportional to the average dose to the particular organ; it does not account for the effect of cell killing in the high dose region, repopulation effect due to fractionation and inhomogeneous dose distribution. Indeed, the non-linear models account for the integral dose and inhomogeneous dose distribution. This approach becomes quite challenging because of a high level of uncertainties in the dose–response models. When interpreting the absolute risk estimates, these uncertainties should be considered. With the extended follow-up data and longer treatment time, one may provide reasonable estimates by considering the general dose distribution characteristics of different plans.

5. Conclusion

The present study indicates that the LAR of SC is lower for all the organs with the institutional 3D conformal matched field method as compared to the IMRT and 3D conformal gap junction methods. Both the institutional 3D conformal field matching method and IMRT have advantages over the traditional gap junction method considering the sparing of organs at risk during CSI. However, the distribution of low dose volume which increases the integral dose of IMRT plan is the main concern for SC risk. At our institute, where 3DCRT is the treatment planning technique of choice, this institutional field matching method is highly robust and ensures easy treatment setup and better long-term prognosis.

Conflict of interest

None declared.

Financial disclosure

None declared.

Acknowledgement

I wish to acknowledge Faculties and staffs of Radiotherapy and Radiological Physics Department of SP Medical College, Bikaner, Rajasthan.

REFERENCES

1. Nell MC, Cot TR, Clegg L, Rorke LB. Incidence and trends in pediatric malignancies medulloblastoma/primitive neuroectodermal tumor; a SEER update. *Med Pediatr Oncol* 2002;**39**:190–4.
2. Monteith SJ, Heppner PA, Wood field MJ, Law AJJ. Pediatric central nervous system tumours in a new Zealand population; a 10 year experience of epidemiology, management and outcomes. *J Clin Neurosci* 2006;**13**:722–9.
3. Suh YI, Koo H, Kim TS. Tumours of the central nervous system in Korea; a multicenter study of 3221 cases. *J Neurooncol* 2002;**56**:251–9.
4. Chan MY, Teo WY, Soow WT, Tan AM. Epidemiology management and treatment outcome of medulloblastoma in Singapore. *Ann Acad Med Singapore* 2007;**36**(5):314–8.
5. Ozek MM, Cinalli G, Maixner W, Rose CS. *Posterior fossa tumors in children*; 2000. New York.
6. Whelan KF, Stratton K, Kawashima T, Waterbor JW, Castleberry RP, Stovall M. Ocular late effects in childhood and adolescent cancer survivors: a report from the childhood cancer survivor study. *Pediatr Blood Cancer* 2010;**54**:103–9.
7. Huang E, Teh BS, Strother DR, Davis QG, Chiu JK, Lu HH. Intensity-modulated radiation therapy for pediatric medulloblastoma: early report on the reduction of ototoxicity. *Int J Radiat Oncol Biol Phys* 2002;**52**:599–605.
8. Merchant TE, Kiehna EN, Li C, Shukla H, Sengupta S, Xiong X. Modeling radiation dosimetry to predict cognitive outcomes in pediatric patients with CNS embryonal tumors including medulloblastoma. *Int J Radiat Oncol Biol Phys* 2006;**65**:210–21.

9. Mertens AC, Yasui Y, Liu Y, Stovall M, Hutchinson R, Ginsberg J. Pulmonary complications in survivors of childhood and adolescent cancer. A report from the Childhood Cancer Survivor Study. *Cancer* 2002;**95**:2431–41.
10. Weiner DJ, Maity A, Carlson CA, Ginsberg JP. Pulmonary function abnormalities in children treated with whole lung irradiation. *Pediatr Blood Cancer* 2006;**46**: 222–7.
11. Hancock SL, McDougall IR, Constine LS. Thyroid abnormalities after therapeutic external radiation. *Int J Radiat Oncol Biol Phys* 1995;**31**:1165–70.
12. Heikens J, Michiels EM, Behrendt H, Endert E, Bakker PJ, Fliers E. Long-term neuro-endocrine sequelae after treatment for childhood medulloblastoma. *Eur J Cancer* 1998;**34**:1592–7 [CrossRef], [PubMed].
13. Green DM, Kawashima T, Stovall M, Leisenring W, Sklar CA, Mertens AC. Fertility of female survivors of childhood cancer: a report from the childhood cancer survivor study. *J Clin Oncol* 2009;**27**:2677–85 [CrossRef], [PubMed].
14. Armstrong GT, Liu Q, Yasui Y, et al. Long-term outcomes among adult survivors of childhood central nervous system malignancies in the Childhood Cancer Survivor Study. *J Natl Cancer Inst* 2009;**101**(13):946–58.
15. Bhatia S, Yasui Y, Robison LL, Birch J, et al. High risk of subsequent neoplasms continues with extended follow-up of childhood Hodgkin's disease: report from the Late Effects Study Group. *J Clin Oncol* 2003;**21**:4386–94.
16. Garwicz S, Anderson H, Olsen JH, Dollner H, et al. Second malignant neoplasms after cancer in childhood and adolescence: a population-based case-control study in the 5 Nordic countries. The Nordic Society for Pediatric Hematology and Oncology. The Association of the Nordic Cancer Registries. *Int J Cancer* 2000;**88**: 672–8.
17. Metayer C, Lynch CF, Clarke EA, Glimelius B, et al. Second cancers among long-term survivors of Hodgkin's disease diagnosed in childhood and adolescence. *J Clin Oncol* 2000;**18**:2435–43.
18. Bhatia S, Sklar C. Second cancers in survivors of childhood cancer. *Nat Rev Cancer* 2002;**2**:124–32.
19. Chaturvedi AK, et al. Second cancers among 104760 survivors of cervical cancer: evaluation of long term risk. *J Natl Cancer Inst* 2007;**99**:1634–43.
20. Hall EJ, Phil D. Intensity-modulated radiation therapy, protons, and the risk of second cancers. *Int J Radiat Oncol Biol Phys* 2006;**65**:1–7.
21. Friedman DL, Whitton J, Leisenring W, Mertens AC, et al. Subsequent neoplasms in 5-year survivors of childhood cancer: the childhood cancer survivor study. *J Natl Cancer Inst* 2010;**102**(14):1083–95.
22. Smith A, Seibel L, Altekruse F, Ries AG, Melbert L, O'Learyet al. Outcomes for children and adolescents with cancer: challenges for the twenty-first century. *J Clin Oncol* 2010;**28**:2625–34.
23. Ng AK, Kenney LB, Gilbert ES, Travis LB. Secondary malignancies across the age spectrum. *Semin Radiat Oncol* 2010;**20**:67–78.
24. Meadows AT, Friedman DL, Neglia JP, et al. Second neoplasms insurvivors of childhood cancer: findings from the Childhood Cancer Survivor Study cohort. *J Clin Oncol* 2009: 27.
25. Zhang R, Howell RM, Giebeler A, Taddei PJ, Mahajan A, Newhauser WD. Comparison of risk of radiogenic second cancer following photon and proton craniospinal irradiation for a pediatric medulloblastoma patient. *Phys Med Biol* 2013;**58**:807–23.
26. *Health risks from exposure to low levels of ionizing radiation: BEIR VII, Phase 2. Estimating cancer risk*. Washington, DC: National Academy of Science; 2006. p. 267–312.
27. Athiyaman H, Mayilvaganan A, Singh D. A simple planning technique of craniospinal irradiation in the eclipse treatment planning system. *J Med Phys* 2014;**39**:251–8.
28. O'Connor MK. Risk of low-dose radiation and the BEIR VII report: a critical review of what it does and doesn't say. *Phys Med* 2017;**43**:153–8.
29. Brenner DJ, Hall EJ. Computed tomography – an interesting source of radiation exposure. *N Engl J Med* 2007;**357**: 2277–84.
30. UNSCEAR: United Nations Scientific Committee on the Effects of Atomic Radiation. *Effects of ionizing radiation. UNSCEAR 2006 Report to the General Assembly, with Scientific Annex United Nations, New York*; 2006.
31. Pagnetti H, Athar S, Moteabad M, Admas A, Schnedider U, Yock I. Assessment of radiation-induced second cancer risks in proton therapy and IMRT for organs inside the primary radiation field. *Phys Med Biol* 2012;**57**: 6047–61.
32. Schneider U, Zwalden D, Ross D, Kaser-Hotz B. Estimation of radiation-induced cancer from three-dimensional dose distributions: concept of organ equivalent dose. *Int J Radiat Oncol Biol Phys* 2005;**61**:1510–5.
33. Brodin NP, Munck AF, Rosenschöld P, Aznar MC, et al. Radiobiological risk estimates of adverse events and secondary cancer for proton and photon radiation therapy of pediatric medulloblastoma. *Acta Oncol* 2011;**50**(6): 806–16.
34. Schneider U, Kaser-Hotz B. Radiation risk estimates after radiotherapy: application of the organ equivalent dose concept to plateau dose–response relationships. *Radiat Environ Biophys* 2005;**44**:235–9.
35. Schneider U, Sumila M, Robotka J. Site-specific dose–response relationships for cancer induction from the combined Japanese A-bomb and Hodgkin cohorts for doses relevant to radiotherapy. *Theor Biol Med Mode* 2011: 8–27.
36. Tatcher M, Glicksman AS. Field matching consideration in craniospinal irradiation. *Int J Radiat Oncol Biol Phys* 1989;**17**(4):865–9.
37. Cheng CW, Das IJ, Chen DJ. Dosimetry in the moving gap region in craniospinal irradiation. *Br J Radiol* 1994;**67**(802):1017–22.
38. Holupka E, Humm J, Tarbell N, Svensson G. Effect of set up error on the dose across the junction of matching craniospinal fields for the treatment of medulloblastoma. *Int J Radiat Oncol Biol Phys* 1993;**27**:345–52.
39. Sharma DS, Gupta T, Jalali R, Master Z, et al. High-precision radiotherapy for craniospinal irradiation: evaluation of three-dimensional conformal radiotherapy, intensity-modulated radiation therapy and helical TomoTherapy. *Br J Radiol* 2009;**82**(984): 1000–9.
40. Mu X, Bjork-Eriksson T, Nill S, et al. Does electron and proton therapy reduce the risk of radiation induced cancer after spinal irradiation for childhood medulloblastoma? A comparative treatment planning study. *Acta Oncol* 2005;**44**:554–62.
41. Kry SF, Salehpour M, Followill D, et al. The calculated risk of fatal secondary malignancies from intensity-modulated radiation therapy. *Int J Radiat Oncol Biol Phys* 2005;**62**: 1195–203.
42. Stokkevåg CH, Engeseth GM, Ytre-Hauge KS, et al. Estimated risk of radiation-induced cancer following pediatric cranio-spinal irradiation with electron, photon and proton therapy. *Acta Oncol* 2014;**53**(8): 1048–57.
43. Mole RH. Dose–response relationships. In: Boice JD, Fraumeni JF, editors. *Radiation carcinogenesis: epidemiology and biological significance*. New York: Raven; 1984. p. 403–20.

44. Wheldon EG, Lindsay KA, Wheldon TE. The dose–response relationship for cancer incidence in a two-stage radiation carcinogenesis model incorporating cellular repopulation. *Int J Radiat Biol* 2000;**76**:699–710.

45. Schneider U, Walsh L. Cancer risk estimates from the combined Japanese A-bomb and Hodgkin cohorts for doses relevant to radiotherapy. *Radiat Environ Biophys* 2008;**47**:253–63.